Performance Evolution of Combined Grid-Forming and Grid-Following Inverters with Different Filtering Mechanisms

Md Nurunnabi, Shuhui Li, Hahnemann Mondal, Yang-Ki Hong, Minyeong Choi, Hoyun Won
Department of Electrical and Computer Engineering
The University of Alabama
Tuscaloosa, AL 35487, U.S.A

Abstract-- This paper discusses the challenges faced by electric power systems due to the increasing use of inverterbased renewable energy resources (IBRs) operating in gridfollowing mode (GFL) and the limited support they provide for the grid's reliability and stability. With increased IBRs connected to the grid, electric utilities are increasingly requiring IBRs to behave like traditional grid-forming (GFM) synchronous generators to provide support for inertia, frequency, voltage, black start capability, and more. The paper focuses on developing GFM inverter technologies with L, LC, and LCL filters and investigates the performance of combined GFM and GFL inverters with different filtering mechanisms when supplying different types of loads. It also emphasizes achieving voltage controllability at the point of common coupling of the GFM with the rest of an AC system. EMT simulation is utilized to investigate the interaction of combined GFM and GFL inverters with different filtering mechanisms. The research results will assist electric utilities in ensuring the reliability and stability of electric power systems in the future.

Index Terms-- Inverter-based renewable energy resources, Grid-forming inverters, Filtering mechanisms, EMT simulation.

I. INTRODUCTION

GRID-FORMING (GFM) inverters have become increasingly important for the operation of electric power systems (EPSs) with the rising deployment of inverterbased resources (IBRs) [1]. Like a traditional synchronous generator, a GFM inverter can provide independent voltage and frequency support to an EPS [2]. Droop control is a well-established method that allows multiple GFM and grid-following (GFL) inverters to operate stably [3]. To connect a GFM inverter to an EPS or microgrid, a coupling filter is mandatory to limit harmonics resulting from the inverter's switching impact [4]. Conventionally, for a GFL inverter, typical coupling filters include L, LC, and LCL filters [5]. However, for a GFM inverter, an LC filter is usually adopted, while L and LCL filters are less common [1], making it important to investigate whether it is possible to build a GFM inverter with all three filtering mechanisms, and if so, how to implement them and what impacts they have on combined GFM and GFL inverters under different filtering mechanism when supplying different types of loads.

Loads in an EPS can be of various types, including R, RL, and RC loads, as well as combinations of all three. Many studies related to GFM inverters have used the same

types of loads as examples in their case studies [6-9]. However, it is crucial to investigate how GFM and GFL inverters behave and present different characteristics when supplying different types of loads, depending on the coupling filter employed [10]. Currently, a comprehensive study has not been conducted to evaluate the performance of combined GFM and GFL inverters with different coupling filters when supplying diverse types of loads. Therefore, this paper aims to investigate some of the special characteristics of combined GFM and GFL inverters and benefit the design of an overall GFM-GFL inverter system by evaluating the impacts of different filtering mechanisms on the system's performance when supplying different types of loads.

To achieve the above objectives, the paper is organized as follows. First, in Section II, we provided a detailed theoretical study on how the GFM output active and reactive powers should be regulated for a GFM using L, LC, and LCL filters. Second, based on the theoretical study obtained and presented in Section II, control strategies for a GFM inverter and a GFL inverter with L, LC, and LCL filters are developed and presented in Section III. In particular, we emphasize the voltage control of the GFM at its output connection point with the AC system instead of the capacitor voltage that was targeted by the conventional methods reported in the literature. Finally, electromagnetic transient simulation (EMT) is conducted in Section IV to give a comprehensive evaluation of the operation, control, and harmonics of combined GFM and GFL inverters under different load types and coupling filtering schemes. Section V gives summary remarks.

II. OUTPUT POWER MODEL OF A GRID-FORMING INVERTER WITH L, LC, AND LCL FILTERS

A. Grid-Forming Inverter

A GFM inverter denotes an inverter having a control approach with the capability to form the grid voltage and frequency purely by inverters without the support of bulk electric generators. A GFM inverter fundamentally behaves as a voltage source behind a coupling filter, as shown in Fig. 1, and controls both the voltage magnitude and the angular frequency preferably at the point of common coupling (PCC) with AC loads or the rest of a larger AC network [11]. At the inverter terminal, the voltage injected to the AC system, e_{abc_inv} , is related to the controller output voltage, $e^*_{abc_inv}$, as follows [12],

$$e_{abc\ inv} = k_{PWM} \cdot e_{abc\ inv}^* \tag{1}$$

where k_{PWM} stands for the ratio of the inverter terminal voltage to the output voltage of the controller caused by the pulse-width modulation (PWM). The coupling filter plays a critical role in designing the controller, eliminating the harmonics resulted from the PWM of the inverter, and determining the ability of the GFM inverter to inject active and reactive power at the PCC. The three typical grid filters are L, LC and LCL filters.

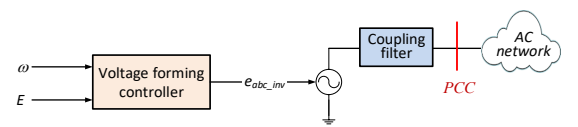


Fig. 1. Conceptual model of a GFM inverter

B. GFM inverter output power at the PCC

In general, the output power at the PCC depends on the inverter output voltage in the AC system, the PCC voltage, and types and parameters of the grid filter. Fig. 2 presents the schematic of a GFM inverter with an LCL-filter, in which L_{inv} and R_{inv} are the inductance and resistance of the inverter-side inductor, C stands for the filter capacitor, L_g and R_g are the inductance and resistance of the PCC-side inductor. The LC and L filters can be considered as a special case of the LCL-filter.

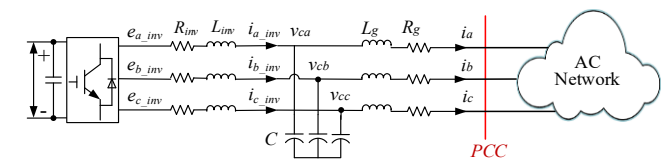


Fig. 2. LCL-filter-based grid-connected converter schematic

Using the generator sign convention and in the steadystate, the voltage balance equation of the inverter-side inductor is

$$\vec{E}_{inv} = R_{inv} \vec{I}_{inv} + j\omega_s L_{inv} \cdot \vec{I}_{inv} + \vec{V}_c = Z_{inv} \vec{I}_{inv} + \vec{V}_c,$$
 (2)

The voltage balance equation of the PCC-side inductor is

$$\vec{V}_c = R_\sigma \vec{I}_{PCC} + j\omega_s L_\sigma \cdot \vec{I}_{PCC} + \vec{V}_{PCC} = Z_\sigma \vec{I}_{PCC} + \vec{V}_{PCC}, \quad (3)$$

The current equation of the LCL capacitor is

$$\vec{I}_{inv} = \vec{I}_{PCC} + j\omega_s C \cdot \vec{V}_c = \vec{I}_{PCC} + j\vec{V}_c / X_c$$
 (4)

where \vec{E}_{inv} , \vec{I}_{inv} , \vec{V}_c , \vec{I}_{PCC} and \vec{V}_{PCC} represent the steady-state phasors of inverter output voltage, current in the inverter-side inductor, capacitor voltage, PCC-side inductor current, and PCC voltage; $Z_{inv} = R_{inv} + j\omega_s L_{inv}$, $Z_g = R_g + j\omega_s L_g$, and $X_C = 1/(\omega_s C)$ stand for the impedances of the inverter-side inductor, PCC-side inductor, and filter capacitor, respectively. Neglect the resistance, the steady state current flowing to the AC network at the PCC can be obtained from (2) - (4), as follows

$$\vec{I}_{PCC} = \frac{\vec{E}_{inv} - \vec{V}_{PCC} \left(1 - X_{inv} / X_c \right)}{j \left(X_{inv} + X_\sigma - X_{inv} X_\sigma / X_c \right)} = \frac{\vec{E}_{inv} - \vec{V}_{PCC_F}}{j X_F}$$
(5)

where $X_F = X_{inv} + X_g - X_{inv} X_g / X_c$ and

 $\vec{V}_{PCC_F} = \vec{V}_{PCC} (1 - X_{inv}/X_c)$. Take \vec{V}_{PCC} as the reference and assume $\vec{E}_{inv} = E_{inv} \angle \delta_{inv}$. Then, the PCC current can be expressed as

$$\vec{I}_{PCC} = \frac{E_{inv} \sin \delta_{inv}}{X_F} - j \frac{E_{inv} \cos \delta_{inv} - V_{PCC_F}}{X_F}$$
 (6)

Thus, the power transferred to the AC network from the GFM inverter at the *PCC* can be obtained from the complex power equation,

$$P_{PCC} + jQ_{PCC} = \vec{V}_{PCC}\vec{I}_{PCC}^* = V_{PCC}\vec{I}_{PCC}^*$$
, as follows

$$P_{PCC} = V_{PCC} \frac{E_{inv} \sin \delta_{inv}}{X_E} \approx \frac{V_{PCC} E_{inv}}{X_E} \delta_{inv}$$
 (7a)

$$Q_{PCC} = V_{PCC} \frac{E_{inv} \cos \delta_{inv} - V_{PCC_F}}{X_E} \approx V_{PCC} \frac{E_{inv} - V_{PCC_F}}{X_E} \quad (7b)$$

The similar active and reaction equations for a GFM inverter with an LC and L filter can be developed except

that
$$X_F = X_{inv}$$
 and $\vec{V}_{PCC_F} = \vec{V}_{PCC} \left(1 - \frac{X_{inv}}{X_c} \right)$ for the LC -

filter GFM inverter, and $X_F = X_{inv}$ and $\vec{V}_{PCC_F} = \vec{V}_{PCC}$ for the *L*-filter GFM inverter. Thus, for a GFM inverter with *L*, *LC* and *LCL* filter, the active power of a GFM inverter injected to the AC network can be controlled by varying the phase angle or frequency of the inverter injected voltage and the reactive power of the inverter injected to the AC network can be controlled by varying the amplitude of the inverter injected voltage according to (7a) and (7b).

III. CONTROL OF GRID-FORMING AND GRID-FOLLOWING INVERTERS

A. Frequency and voltage control of a GFM Inverter

Conventionally, two typical control configurations are a GFM controller with and without a current control loop, in which the GFM controller without a current control loop is more reliable according to [9] and is used in this paper for the development and evaluation of a GFM inverter with *L*, *LC*, and *LCL* filters. According to the analysis shown in Section II, the active and reactive powers at the *PCC* can be regulated by controlling the frequency and voltage amplitude of the inverter-injected voltage. Therefore, the injected voltage of the GFM inverter with any one of the *L*, *LC*, and *LCL* filters is generated as follows:

$$\theta_{inv}(t) = \int_0^t 2\pi f^*(\tau) d\tau \tag{8a}$$

$$E_{inv}(t) = k_p \left(V_{PCC}^*(\tau) - V_{PCC}(\tau) \right) + k_i \int_0^t \left(V_{PCC}^*(\tau) - V_{PCC}(\tau) \right) d\tau$$
(8b)

$$e_{inv}^{a}(t) = E_{inv}(t)\sin(\theta_{inv}(t))$$
(8c)

in which the instantaneous angle of the injected voltage is calculated by (8a) based on the desired reference frequency f^* , the instantaneous amplitude of the injected voltage is calculated by (8b) via a PI control mechanism, and (8c) shows the phase-a of the instantaneous injected voltage. In (8b), V_{PCC}^* is the reference PCC rms line voltage and V_{PCC} is the actual PCC rms line voltage. Therefore, different from the GFM inverters developed previously by others, our objective is to maintain the stability and controllability of the PCC voltage instead of the capacitor voltage for an LC-filter GFM inverter. The reference frequency and rms line voltage of the voltage at the PCC are generated through a droop control mechanism as explained below.

The droop control is the outer loop control after the frequency and voltage control loop and contains two droop controllers, a P-f droop control and a Q-V droop control. The P-f droop controller generates the reference frequency according to (9) and the Q-V droop controller generates the reference rms line voltage according to (10).

$$f_{i}^{*}(t) = f_{0} + R_{fi}(P_{i}^{*}(t) - P_{i}(t))$$
(9)

$$V_{i}^{*}(t) = V_{0} + R_{Vi}(Q_{i}^{*}(t) - Q_{i}(t))$$
(10)

In (9), $f_i^*(t)$ represents the reference frequency of the i's GFM inverter output voltage generated by the P-f droop controller at time t, f_0 represents the nominal frequency of the AC network, R_f is the frequency droop coefficient, and $P_i^*(t)$ and $P_i(t)$ represent the desired and locally measured active power of the ith GFM inverter at time t, respectively. In (10), $V_i^*(t)$ represents the reference PCC rms line voltage of the i's inverter at time t, V_0 represents the nominal PCC rms line voltage of the AC network, R_f is the voltage droop coefficient, and $Q_i^*(t)$ and $Q_i(t)$ represent the desired and locally measured reactive power of the ith GFM inverter at time t, respectively. Fig. 3 illustrates the developed droop control concept for a GFM inverter.

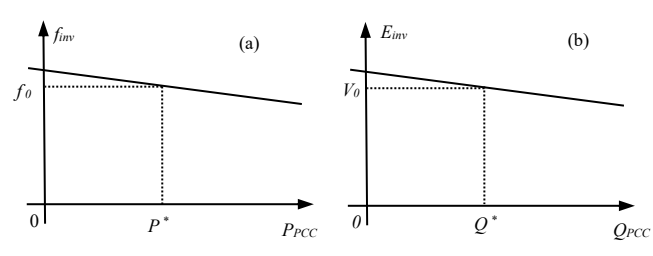


Fig. 3. P-f droop and Q-V droop of a GFM inverter

B. Active and reactive power control of a GFL Inverter

A GFL inverter generally has a cascaded outer-loop active power and reactive power controller plus an inner-

loop current controller, typically designed in the d-q reference frame based upon the PCC voltage orientation with the grid. The active and reactive power controller in the outer-loop produces d-axis and q-axis current references and the current controller in the inner-loop produces d-axis and q-axis control voltage signals, $v^*_{d_i inv}$ and $v^*_{q_i inv}$. At the inverter terminal, the voltage injected to the grid, $v_{dq_i inv}$, is related to the controller output voltage as $v_{dq_i inv} = k_{PWM} \cdot v^*_{dq_i inv}$, where k_{PWM} stands for the PWM ratio between the inverter terminal voltage and the output voltage of the controller.

For GFL inverters operating with GFM inverters in islanded conditions, such as a microgrid, droop control is important and needed for a GFL inverter too. The droop control loop should be an external control loop after the active and reactive power control loop and contains a f-P droop control and a V-Q droop control. The f-P droop controller generates the active power reference according to (11) and the V-Q droop controller generates the reactive power reference according to (12).

$$P_{i}^{*}(t) = P_{i}^{set}(t) + M_{fi}(f_{0} - f_{i}(t))$$
(11)

$$Q_{i}^{*}(t) = Q_{i}^{set}(t) + M_{Vi}(V_{0} - V_{i}(t))$$
(12)

where M_{f} is the f-P droop coefficient and M_{V} is the V-Q droop coefficient, Fig. 4 illustrates the developed droop control concept for a GFL inverter.

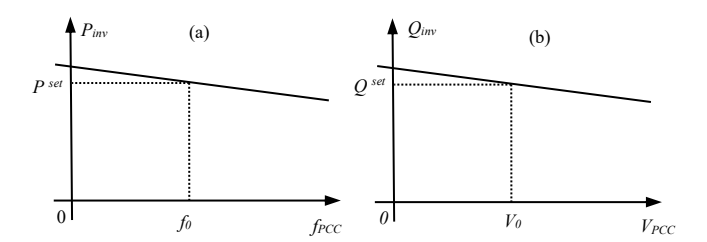


Fig. 4. f-P droop and V-Q droop of a GFM inverter

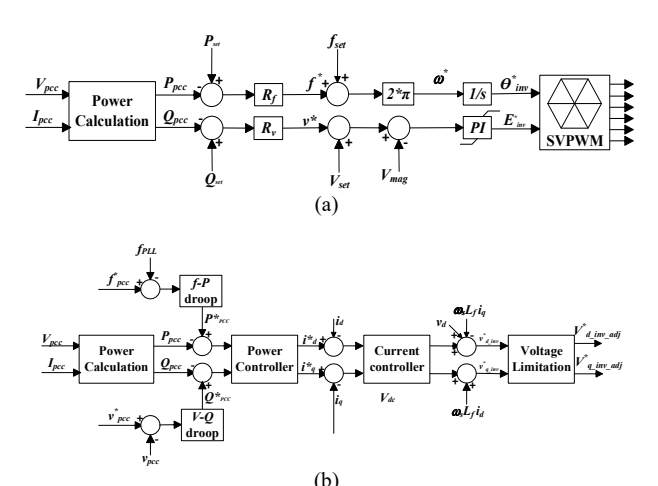


Fig. 5. Overall control configuration for (a) GFM inverter and (b) GFL

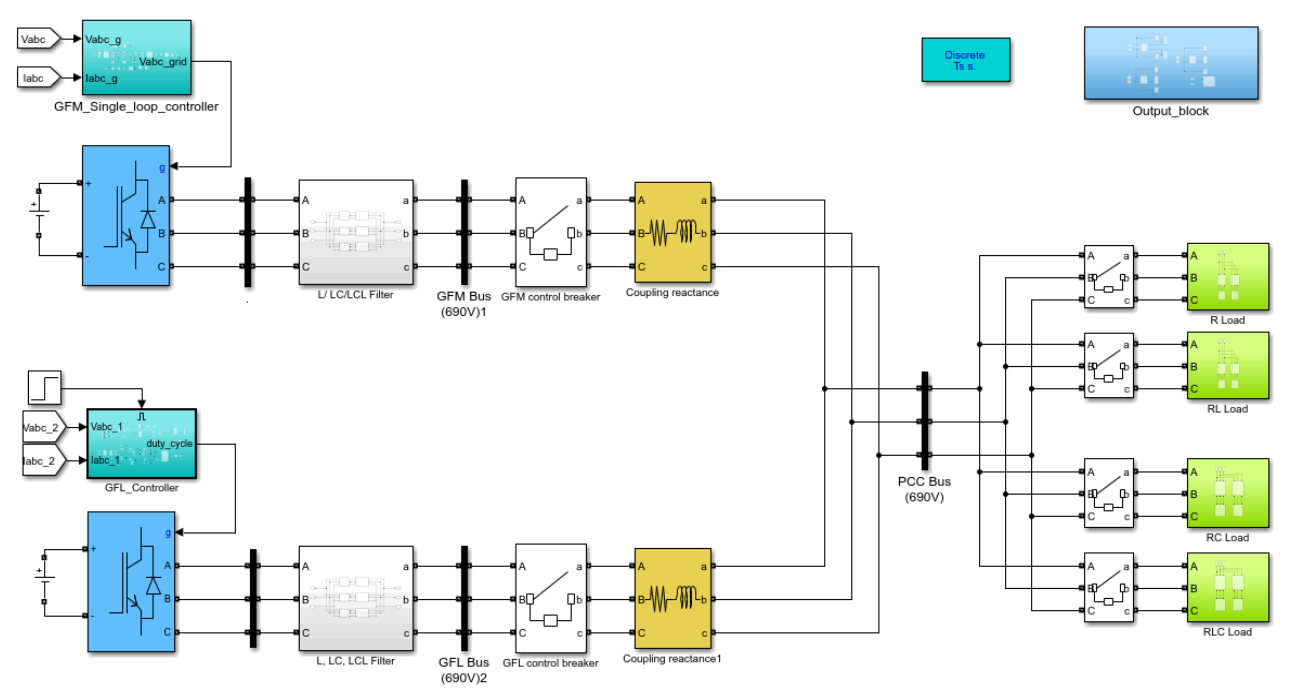


Fig. 6. EMT simulation model of a GFM with a GFL inverter

C. Overall GFM and GFL control configurations

Fig. 5a shows the overall control configuration suitable for a GFM inverter with L, LC, and LCL filters. The droop control loop generates the frequency and rms voltage references to the frequency and voltage control loop. The frequency and voltage loop generates inverter output voltage according to (8). A saturation mechanism is applied to the PI voltage controller to prevent the integral term of the PI controller from going beyond the maximum possible output voltage limit of the GFM inverter.

Fig. 5b shows the overall control configuration suitable for a GFL inverter with L, LC, and LCL filters. The droop control loop generates the active and reactive power references to the active and reactive power control loop. The active and reactive power control loop generates the dq current references to the current loop controller, and the current loop controller generates the inverter output voltage based on the PWM.

IV. CONTROL AND OPERATION EVALUATION OF COMBINED GFM AND GFL INVERTERS VIA EMT SIMULATION

A. EMT simulation model

To evaluate the performance of combined GFM and GFL inverters with L, LC, or LCL filter, an EMT simulation model of the GFM and GFL system with loads is developed that is shown in fig. 6. The following parameters are used as the nominal values for both the GFM and GFL inverters. 1) The inverter-rated power is 100kVA. 2) The dc-link voltage is 1300V. 3) The PCC line voltage is 60Hz, 690V rms. 4) For the L filter, the inductance is 4mH and the resistance of the inductor is 0.012Ω . 5) For the LC filter, the inductor remains the

same, and the capacitance is $25\mu F.$ 6) For the LCL filter, the capacitance is the same as that of the LC filter while the inductance is 2mH and the resistance of the inductor is 0.006Ω for both the inverter- and grid-side inductors. Then, the performance of the combined GFM and GFL inverter system is investigated by considering different scenarios.

B. Operation of GFM and GFL inverters

In this case, a GFM and GFL simulation model is built in which a GFM inverter and a GFL inverter are connected in parallel to supply loads. An LCL filter is applied to both inverters, which can be easily modified as an LC or L filter. The rated capacity and the rated line voltage of the GFL inverter are the same as those of the GFM inverter shown in Section IV-A. The GFM inverter intends to maintain the voltage stability with low voltage THD at the PCC while the GFL inverter tries to control the current injected into its PCC with low current THD. The different objectives of the two make it more challenging than a simple GFM case. Basically, when the GFL is added, both fundamental and harmonic currents of the GFL would affect the reliability and distortion of the load bus voltage. This certainly would increase the difficulty for the GFM to maintain a stable and sinusoidal PCC voltage.

Fig. 7 shows the operation of a GFM with a GFL inverter to supply an RL load of 70kW/70kVar, in which an LCL filter is applied to both GFM and GFL inverters. The filter parameters are the same as those used in previous sections. Before t=1sec, the load is supplied by the GFM only and the PCC voltage and current are well maintained with good power quality. After t=1sec when the GFL is added to provide a part of the active/reactive power to the load, a higher PCC voltage and current distortion is shown. This situation is worse when other types of grid-connected filters, L and LC filters, are

applied to the GFM and GFL inverters. Overall, the results show that the introduction of the GFL inverters could result in more reliability and harmonic issues and the adoption of appropriate inverter filters is critical for the high performance of the integrated GFM and GFL inverter operation.

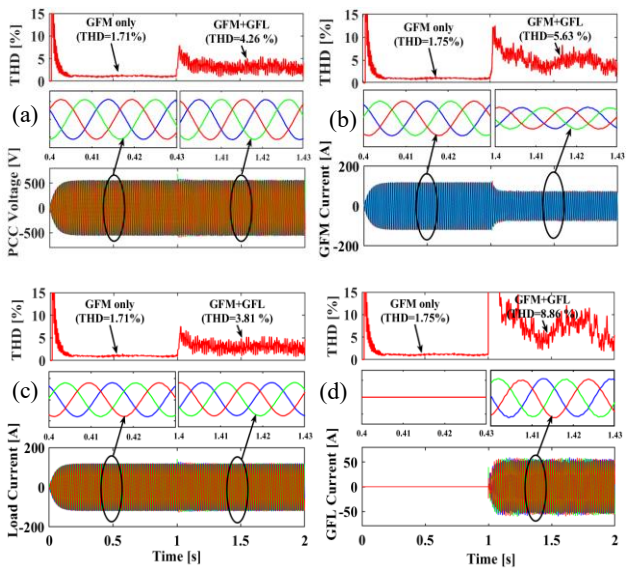


Fig. 7. GFM and GFL supplying an RL load (70kW, 70kVAR) where 50% load is supplied by the GFM and the rest supplied by the GFL. (a) PCC voltage (b) GFM current (c) Load current (d) GFL current.

C. Operation of combined GFM and GFL inverters supplying a varying load

The operation of GFM and GFL inverters was evaluated under varying load conditions. The case studies examined the performance of GFM and GFL inverters, which were tasked with supplying a distinct load with different ratios of R, RL, and RC over time. Specifically, the GFM inverter supplied 50% of the load while the GFL inverter supplied the remaining power. The output of this case studies is shown in Figure 8.

Notably, the GFM inverter was found to be capable of maintaining the load voltage stability at a constant level despite significant variations of the load over time. For instance, when the load dropped by 80%, the inverter was able to recover the line voltage immediately.

The performance of both the GFL and GFM inverters was found to slightly decline when supplying low power demands in terms of the total harmonic distortion (THD). Nevertheless, both inverters were able to maintain a THD level below 4% even with variations in the load types supplied by the combined GFM and GFL inverters. However, it was observed that the THD performance deteriorated a little bit when supplying low loads, which is consistent with the traditional GFL inverter performance under low load conditions.

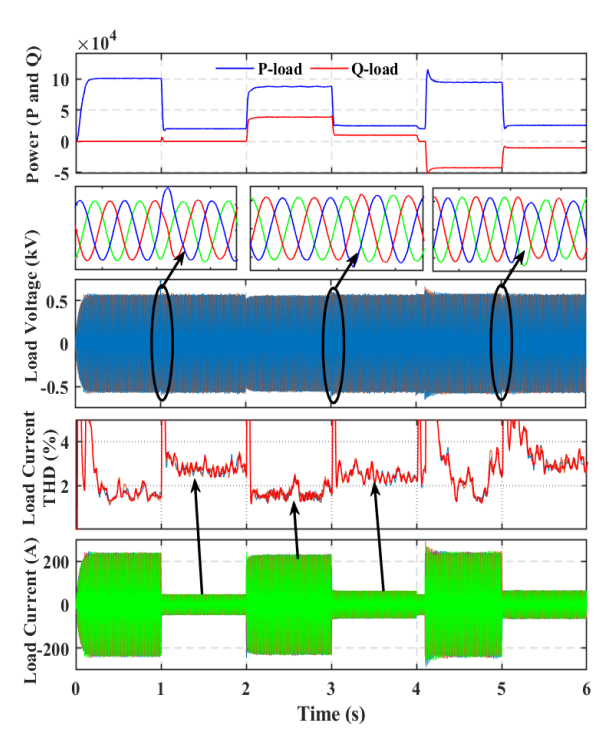


Fig. 8. GFM and GFL supplied a distinct load with different ratios of R, RL, and RC, where the GFM inverter supplied 50% of the load and the GFL inverter supplied the remaining 50%.

D. Operation of combined GFM and GFL inverters for different power sharing ratio between inverters

When GFM and GFL inverters operate together, the GFM inverter establishes the voltage and frequency of the ac system while the GFL inverter operates based on the voltage and frequency built by the GFM inverter. When the power supplied by the GFL inverters increase, voltage and frequency stability of the ac system is certainly an important issue to look at.

Fig. 9 shows the combined GFM and GFL inverters supplying a resistive load with different power sharing ratios between the two inverters. The power sharing ratio of the GFM inverter starts from 100% at t=0sec to 50% and less after t=5sec. From the figure, we can observe that the GFM and GFL inverters operate at varying levels of the power sharing between the two inverters when a resistive load is present. As we examine the figure more closely, we can see that as the contribution of GFM decreases, the current THD of the load increases. Conversely, as the contribution of GFL increases to support the load, the current THD decreases. Additionally, it is noteworthy that the GFL can only inject up to 50% power into the system before the system becomes highly distorted or even unstable.

Furthermore, we can deduce that a higher ratio of GFM provides superior performance of the system. It is important to keep in mind that the results obtained in this experiment were under a resistive load and may vary under different load conditions.

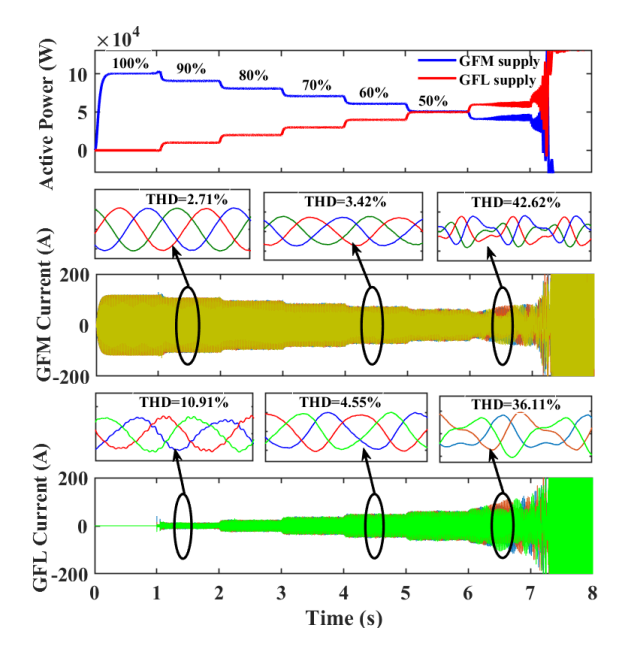


Fig. 9. The GFM and GFL inverters operating at different ratios of GFL and GFM Inverter penetration. It is evident from the figure that the GFL can inject a maximum of 50% power into the system.

V. CONCLUSIONS

With increased invert-based resources connected to the electric power grid, demand for inverter-based renewable energy sources to have the GFM capability is increasing. Traditionally, a GFM inverter is connected to the grid through an LC filter and the voltage at the capacitor is controlled. This paper investigates the potential of building a GFM inverter with L, LC, and LCL filters and controlling the PCC voltage instead of the capacitor voltage of the GFM system. The paper shows a theoretical analysis of how the PCC voltage can be maintained by the GFM using the three different filtering schemes. Then, the paper focuses on a detailed performance evaluation of combined GFM and GFL inverter system considering L, LC, or LCL filter applied to both types of inverters. The study shows that the combined GFM and GFL system is more reliable and has high performance when an LCL filter is used to both types of inverters. Within its rated current and PWM saturation limits, the GFM and GFL combination with L, LC, or LCL filter can maintain frequency and voltage stability and high-power quality under a variety of loads and load variation conditions. However, when the GFL inverters dominate the load sharing, the risk of the system distortion and stability becomes high.

ACKNOWLEDGMENT

This work is supported by the National Science Foundation, U.S.A. The grant numbers supporting the work are 2137275 and 2141067.

REFERENCES

- [1] R. H. Lasseter, Z. Chen and D. Pattabiraman, "Grid-Forming Inverters: A Critical Asset for the Power Grid," in IEEE Journal of Emerging and Selected Topics in Power Electronics, vol. 8, no. 2, pp. 925-935, June 2020, doi: 10.1109/JESTPE.2019.2959271.
- [2] X. Quan et al., "Photovoltaic Synchronous Generator: Architecture and Control Strategy for a Grid-Forming PV Energy System," in IEEE Journal of Emerging and Selected Topics in Power Electronics, vol. 8, no. 2, pp. 936-948, June 2020, doi: 10.1109/JESTPE.2019.2953178.
- [3] Teng, Y., Deng, W., Pei, W., Li, Y., Dingv, L., & Ye, H. (2022). Review on grid-forming converter control methods in high-proportion renewable energy power systems. Global Energy Interconnection, 5(3), 328-342. https://doi.org/10.1016/j.gloei.2022.06.010
- [4] Lin, Yashen, Joseph H. Eto, Brian B. Johnson, Jack D. Flicker, Robert H. Lasseter, Hugo N. Villegas Pico, Gab-Su Seo, Brian J. Pierre, and Abraham Ellis. 2020. Research Roadmap on Grid-Forming Inverters. Golden, CO: National Renewable Energy Laboratory. NREL/TP-5D00-73476. https://www.nrel.gov/docs/fy21osti/73476.pdf.
- [5] U. P. Yagnik and M. D. Solanki, "Comparison of L, LC & LCL filter for grid connected converter," 2017 International Conference on Trends in Electronics and Informatics (ICEI), Tirunelveli, India, 2017, pp. 455-458, doi: 10.1109/ICOEI.2017.8300968.
- [6] J. Hernandez-Alvidrez, N. S. Gurule, M. J. Reno, J. D. Flicker, A. Summers and A. Ellis, "Method to Interface Grid-Forming Inverters into Power Hardware in the Loop Setups," 2020 47th IEEE Photovoltaic Specialists Conference (PVSC), Calgary, AB, Canada, 2020, pp. 1804-1810, doi: 10.1109/PVSC45281.2020.9300804.
- [7] R. Mittal and Z. Miao, "Analytical Model of A Grid-Forming Inverter," 2022 IEEE Power & Energy Society General Meeting (PESGM), Denver, CO, USA, 2022, pp. 1-5, doi: 10.1109/PESGM48719.2022.9916676.
- [8] R. Mittal, Z. Miao and L. Fan, "Grid Forming Inverter: Laboratory-Scale Hardware Test Bed Setup and Weak Grid Operation," 2021 North American Power Symposium (NAPS), College Station, TX, USA, 2021, pp. 1-6, doi: 10.1109/NAPS52732.2021.9654589.
- [9] W. Du et al., "A Comparative Study of Two Widely Used Grid-Forming Droop Controls on Microgrid Small-Signal Stability," in IEEE Journal of Emerging and Selected Topics in Power Electronics, vol. 8, no. 2, pp. 963-975, June 2020, doi: 10.1109/JESTPE.2019.2942491.
- [10] S. C. Verbe, R. Shigenobu and M. Ito, "Comparative Study of GFM-grid and GFL-grid in Islanded Operation," 2021 IEEE PES Innovative Smart Grid Technologies - Asia (ISGT Asia), Brisbane, Australia, 2021, pp. 1-5, doi: 10.1109/ISGTAsia49270.2021.9715619.
- [11] A. Singhal, T. L. Vu and W. Du, "Consensus Control for Coordinating Grid-Forming and Grid-Following Inverters in Microgrids," in *IEEE Transactions on Smart Grid*, vol. 13, no. 5, pp. 4123-4133, Sept. 2022, doi: 10.1109/TSG.2022.3158254.
- [12] N. Mohan, Advanced Electric Drives, John Wiley & Sons, ISBN 978-1-118-48548-4, 2014.